

Numerical Simulation and Design of Friction-Damped Steel Frame Structures

J.D. Morales Ramirez

*Former Graduate Student Concordia University, Montreal, Canada
Civil Department SNC-Lavalin T & D, Calgary, Canada*

L. Tirca

Concordia University, Montreal, Canada



SUMMARY: (10 pt)

During the last decades, a large number of energy dissipating devices were developed, whereas pioneering work on friction dampers was firstly reported by Pall (1979). Existing numerical models of friction devices are based on hysteretic model that uses elasto-plastic representation and follows the Coulomb's friction law. However, the structural system with friction devices is highly nonlinear due to the kinematic conditions of slip and stick phases of device behaviour, as well as the transition stages from elastic to slipping (stick-slip phase) and from slipping to failure (slip-lock phase) either in bearing or bolt shearing. To have an accurate model of friction devices, all these behavioural phases should be incorporated. Thus, to overpass the drawback regarding friction damper modelling, an equivalent material is proposed in the OpenSees environment. Nonlinear time-history analyses of a 8-storey MRF building equipped with friction-damped braces are carried out.

Keywords: Friction damper, Slip-lock phase, OpenSees model, BoucWen material, Slip distance.

1. INTRODUCTION

In the aim to reduce the inelastic demand triggered in structural members of frame buildings during seismic excitations, innovative cost-efficient solutions have been proposed by researchers. Accordingly, by adding supplemental damping to a structural system, the damage energy is reduced and the inelastic response of earthquake resistant members is controlled. In general, damping can be added by incorporating passive and active energy dissipaters. Pioneering work on friction devices, designed to dissipate energy through the relative sliding of plates clamped by post-tensioned bolts, was conducted by Pall (1979) and Pall and Marsh (1981). Thus, the purpose of installing friction dampers in a frame system is to activate the Coulomb damping that is generated when the friction mechanism is developed due to the attainment of slip forces under specified lateral deformations.

The reported static and dynamic tests conducted by Pall (1979) on several sliding elements with different surface treatments, emphasised the benefit of using friction devices due to their capacity of generating rectangular hysteresis loops. The considered surface treatments and the response of slip bolted joints under monotonic loading are shown in Fig. 1.1a and correspond to a normal force that was applied by pretensioning 12.7 mm diameter high strength bolts. Pall has reported that the most stable behaviour under static and dynamic loading was obtained when brake lining pads in contact with mill scale surface on plate was chosen. During the cyclic tests, the hysteretic behaviour did not show appreciable degradation, which means that the friction device has the capacity to develop uniform friction coefficient. Nevertheless, a minor difference between the static and dynamic friction coefficient remained. As illustrated in Fig. 1.1a, under large seismic excitations, the post-tensioned bolts of friction dampers may undergo an additional stage following sliding that is characterised by bearing of bolts or even shear failure. In this stage, a sudden increment in storey shear force accompanied by decreasing of Coulomb damping is encountered. A similar behaviour to that of an elasto-perfectly plastic system was identified (Fig. 1.1b) and the back-bone curve is composed of four stages: elastic, slipping, bearing and bolt shear failure. From the back-bone curve illustrated in Fig.

1.1b, is shown that the length of the slotted hole controls the slip distance. When cyclic quasi-static loading was applied, the hysteresis behaviour showed symmetrical rectangular loops (Fig. 1.1c) which are largely influenced by the fluctuation of friction coefficient during the slipping stage. Herein, the maximum force is the slip load and the maximum displacement is half length of slotted hole. However, transitory changes between adjacent stages were not simulated. These shortcomings were documented in studies conducted by Roik et al. (1988) and Lukkunaprasit et al. (2004).

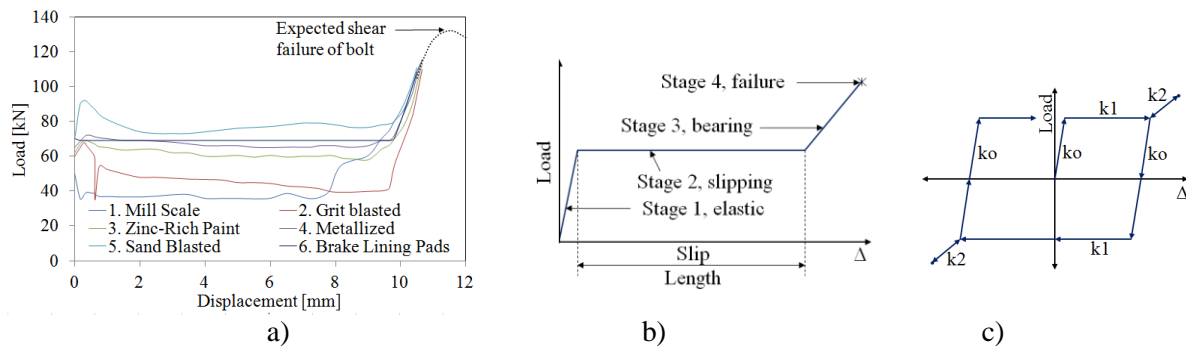


Figure 1.1. Response of slip bolted joint: a) monotonic test, b) back-bone curve, c) hysteretic behaviour (after A. Pall, 1979)

Experimental and analytical studies conducted by Roik et al. (1988) on slotted bolted connections emphasized the occurrence of bearing stage due to the bolt impact that arose when the slip demand is larger than the available length of slotted hole. Later on, Lukkunaprasit et al. (2004) investigated the behaviour of slotted bolted connections subjected to cyclic loading, before and after the available slip distance was reached. The results showed that the bolt impact comprises a nonlinear additional stage added to the customary rectangular hysteretic loop. As a consequence, the energy dissipation amount was diminished, while the hysteresis shape was reduced due to a repeating exceedance of slip distance throughout cycles. It was noted that this jump in force resistant at bearing is limited by the shearing capacity of the high strength bolts. In addition, when the bearing phase is encountered, an incremented base shear is experienced by the system. Thus, the behaviour of friction devices can be divided in three phases: “stick-slip” before sliding occurs, “slipping”, and the “slip-lock” when bearing is activated.

On the topic of modelling friction dampers, previous studies have considered only elasto-plastic models. Lukkunaprasit et al. (2004) emphasized that these models do not incorporate transitory phases (stick-slip and slip-lock), as well as the option of device decoupling from the structure, when failure occurs. In addition, the current provisions of NBCC 2010 and CAS/ S16-2009 do not provide guidelines regarding earthquake resistant structures equipped with friction devices. Although FEMA 356 (2000) contains some design recommendations as: “all energy dissipation devices shall be capable of sustaining displacements equal to 130% of the maximum calculated displacement in the device” when subjected to ground motions, it does not stipulate design provisions.

Thus, this study is twofold: i) to develop an accurate model for friction dampers that is able to simulate all nonlinear stages using OpenSees software and ii) to emphasize the behavior of middle-rise moment resisting frames (MRF) buildings equipped with friction dampers under seismic excitations.

2. BEHAVIOUR AND SIMULATION OF FRICTION DEVICES

The hysteresis model proposed in this study is able to simulate the behavior of a friction device that is incorporated in a single diagonal tension-compression brace and is subjected to seismic loading. The gradual transition in the vicinity of sharp changes in slope within different phases is considered. However, the OpenSees model proposed herein does not account for degradation during sliding. The experimental tests conducted by Aiken et al. (1993) referred to the behavior of a 9-storey MRF

equipped with Pall friction dampers incorporated in X-bracing system. However, the behavior of a friction-damped tension-compression diagonal brace (FDDB) employed in this study may differ in several aspects. In this light, earlier experimental studies reported by Pall (1979) were considered to calibrate the back-bone curve of friction dampers. The smooth Bouc-Wen hysteresis model is employed, while the stick-lock stage mentioned before is embedded by assigning a set of material objects acting in parallel and playing the role of nonlinear restrainers. Their purpose is to simulate the plastic behavior of the bearing stage that may be encountered during strong earthquake excitations.

2.1. Slipping Stage

During the slipping stage within the available slip distance, the hysteresis shape of friction devices is characterized by the Coulomb friction law. Herein, possible fluctuations in the friction coefficient are neglected. In this regard, a smooth hysteresis model (SHM) which is based on the modified version proposed by Wen (1980) of the strong-nonlinear oscillator model developed by Bouc (1967) is considered. The Bouc-Wen model (BW) is able to simulate the high nonlinear Coulomb friction and has the ability to represent different hysteresis shapes according to the values of the parameters involved. Since the desired shape of the Coulomb dry friction law is symmetric and degradation is neglected, the Bouc-Wen model is reduced to a nonlinear restoring force of a single degree of freedom (SDOF) system shown in Fig. 2.1 and defined by Eqn. 2.1, while the evolutionary variable z evolves as per Eqn. 2.2.

$$f_s(\dot{u}, z) = \alpha k_o u + (1 - \alpha) k_o z \quad (2.1)$$

$$\dot{z} = \dot{u} \left\{ \frac{A - |z|^n [\gamma + \beta \operatorname{sgn}(\dot{u}z)] v}{\eta} \right\} \quad (2.2)$$

Herein, α is the participation ratio of the initial stiffness in the nonlinear response, k_o is the initial stiffness of the system, u is the displacement of the SDOF system and z is the hysteresis variable. In Eqn. 2.2, γ and β are parameters controlling the shape of the hysteresis cycle and the exponent n influences the sharpness of the model in the transition zones. The remaining parameters A , v and η control the degradation process in stiffness and strength. When the degradation process is neglected, the aforementioned parameters are: $A = A_o$, $v = 1$, $\eta = 1$. The considered SDOF system is characterized by the restoring force $f_s (du/dt, z)$ that has a linear and a nonlinear component, as defined in Eqns. 2.1 and 2.2. Knowing that the evolutionary variable z is bounded as shown in Fig. 2.1 and the initial stiffness in the z - u plane can be derived from Eqn. 2.1, the displacement u_y at which the maximum value of z (z_u) intersects the tangent of the response (initial stiffness) is expressed in Eqn. 2.3. The correspondence between the z - u and f_s - u planes is explained by Foliente (1993).

$$u_y = \frac{z_u}{A_o} \rightarrow u_y = \frac{1}{A_o} \left[\frac{A_o}{\gamma + \beta} \right]^{1/n} \quad (2.3)$$

Choosing $A_o = 1$ for the case when the initial stiffness of the hysteresis cycle is equal to the stiffness of the system in the elastic range, the previous Eqn. 2.3 is reduced to:

$$\gamma + \beta = \frac{1}{u_y^n} \quad (2.4)$$

where $u_y = f_{sy}^*/k_o$. Thus, parameters γ and β given in Eqn. 2.4 may be adjusted in accordance with the physical properties of the system (f_{sy}^* is the yielding or activation force and k_o the initial stiffness), the smoothness level at transition zones (n), and the tendency of the tangent stiffness during the loading and unloading stages. For systems with loading stages showing softening and unloading stages with linear trend, the sum of γ and β shall be positive ($\gamma + \beta > 0$) and the difference $\gamma - \beta = 0$ or $\gamma = \beta$. A parametric study was conducted by Morales Ramirez (2011) with the aim to find an optimal value of parameter n . Thus, for $n = 1$ the tendency is to underestimate the restoring force and produce larger

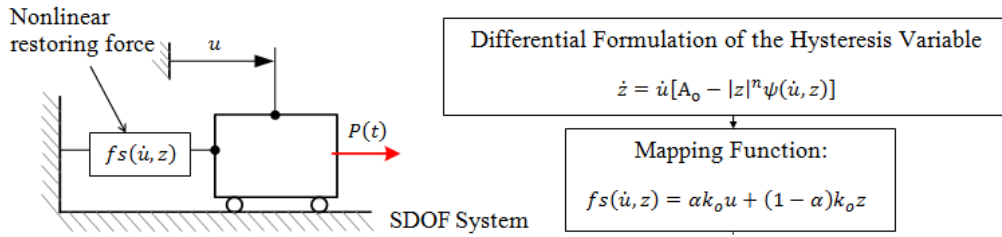


Figure 2.1. SDOF system employed to define the Bouc-Wen model

displacement when comparing with $n = 5$, $n = 10$ and $n = 20$. Hence, using $n = 1$ might yield to a flexible behavior, enlarging the period of vibration and reducing the inertial forces. The smooth transition toward a rectangular hysteresis shape is obtained for a large value of variable n which might become computationally expensive, because the transient analysis requires the calculation of the evolutionary variable z at each step of time for a single element. By using $n = 10$, it gives an acceptable level of prediction because the difference is quickly reduced throughout the evolution of the slipping stage. Thus, the BW model is able to approximate the nonlinearities developed during the transition stage when the system evolves from the elastic to slipping phase.

2.2. Bearing stage

When lateral loads are still acting after the friction device has consumed the available slip distance, the post-tensioned bolts behave as restrains and may evolve from an initial elastic behavior (bolt impact) to an inelastic stage due to bearing of slotted holes and/or bolts. There are not experimental tests conducted for friction devices (e.g. Pall friction dampers) with the aim to investigate the behaviour of the device after the slip limit was exceeded. However, results based on monotonic tests of limited slip bolted joints illustrated in Fig. 1.1 and those obtained by Lukkunaprasit et al. (2004) under cyclic loading, revealed an additional bearing stage that should be added to the backbone curve.

The scope of this work is to provide a hysteresis model able to simulate a smooth transition between the elastic and slipping stage, as well as to incorporate the bearing stage that may happen under strong seismic excitation. To simulate a gradual transition from the time when the slotted plate began to bear against the bolts until failure of bolts occurred, a set of gap-hook elements is used to model the slip-lock stage. In Fig. 2.2 is illustrated a simplified model of friction damper.

From Fig. 2.2 is shown that the axial force transferred from the brace to the friction device produces interface damping due to the Coulomb dry friction developed between the sliding mass and the stationary body (Roberts and Spanos 1990). Thus, the energy dissipated by the device is attributed to friction of the sliding mass and under extreme loads to friction and bearing due to the inelastic action of the bolts that may be encountered when the displacement demand is larger than the available slip distance. Therefore, the slip-lock transition phase can be simulated by a set of elements able to provide gradual transition from the point when the sliding mass impacts the bolt ($u = u_a$) until failure occurs. The point representing force-displacement peers in the slip-lock stage belong to a curve depicted in Fig. 2.3. It encounters sharp changes in the slope during the nonlinear response. Thus, in order to build this behavioural curve, the following points should be defined: the slip force, P_s and the available slip distance, u_a (u_a, P_s); the point characterized by changes in behavior from elastic to plastic, when the slotted plate begin to bear against bolts (u_b, f_b); an intermediate point within the plastification process (u_c, f_c) and the threshold point reached before a drop in the force occurred while the displacement is increased (u_d, f_d). To define these values, experimental tests results are required for an accurate calibration. In this regard, to simulate the bearing stage when the demand is larger than the available slip distance, a set of 6 gap-hook elements (3 in tension and 3 in compression) may be used. A symmetric response is assumed to occur in tension and compression.

In Fig. 2.4 is illustrated a schematic model of a FDDDB device. The behavior of the brace member is

represented by a linear model with the axial stiffness equal to the elastic stiffness of the element. The components acting in parallel (springs 1, 2 and 3) simulate the behavior of a friction device that acts in series with the elastic brace (spring 4). Regarding the friction damper model, the axial springs 1 and 2 simulate the linear and nonlinear component of the BW model, while the spring 3 simulates the slip-lock phase.

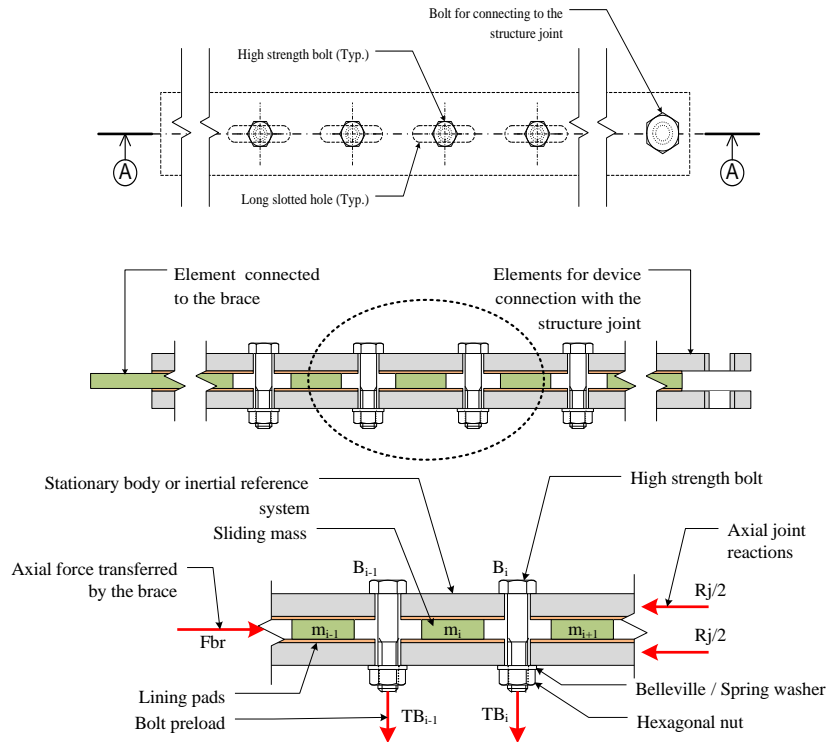


Figure 2.2. Schematic arrangement of one row of high strength bolts of a friction device: a) plan view, b) transversal section of bolts and connected plates c) Detail of the main elements considered in the sliding process

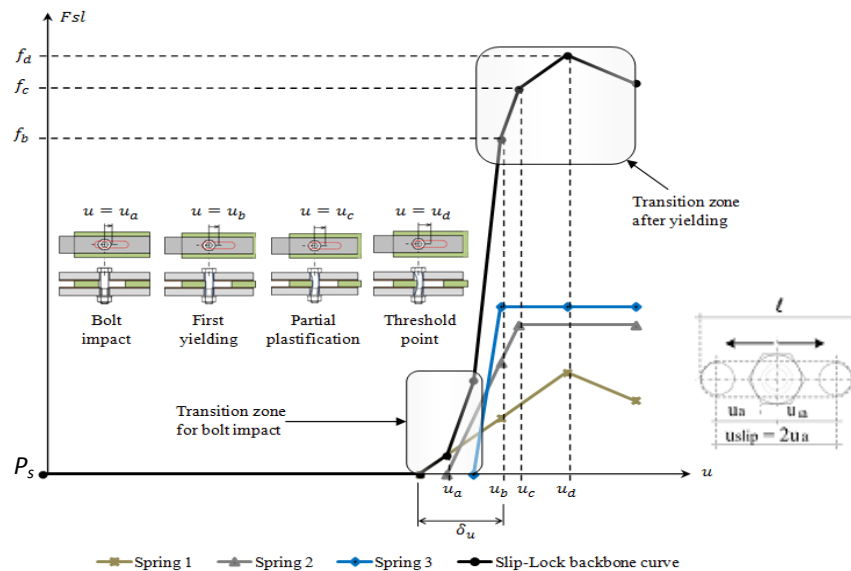


Figure 2.3. The simulation of the slip-lock phase

2.3 Modelling the friction device in OpenSees environment

To simulate the friction-damped diagonal-brace device (FDDB) in OpenSees environment (McKenna et al. 2004), Morales Ramirez (2011) proposed an equivalent uniaxial material composed of different

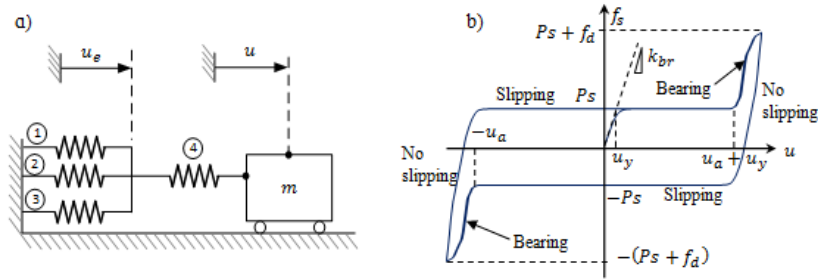


Figure 2.4. Friction device: a) Mechanical model; b) Hysteresis model with bearing phase incorporated

materials that are already available in the OpenSees library and is shown in Fig. 2.5a. This proposed computer model was not considered in previous reported numerical simulations. Herein, the uniaxial *BoucWen* material was selected to replicate the smooth hysteresis behavior (SHB) of friction damper (stick-slip and slipping phase) and was assigned to the truss element. The friction damper is activated when the stress related to the slip force, P_s , defined as $\sigma_s = P_s/A_{br}$ (A_{br} is the gross area of the brace) is reached. The components (2) and (3) are acting in parallel with the *BoucWen* material and are assigned to model the slip-lock phase of the system. They are made of 3 bilinear gap springs arranged in parallel and characterized by the Elastic-Perfectly Plastic Gap material (*ElasticPPGap*). Each uniaxial *ElasticPPGap* material has a defined stress-strain or force-deformation relationship either in tension or in compression to model the bearing of the bolt. Thus, the second component (2) is activated in tension when the displacement demand exceeds the available slip distance, u_a . Once activated, this component is able to limit the displacement and to increase the force experienced by the diagonal-brace with friction damper incorporated. The third component (3) is similar to (2), but is activated in compression when the travel distance u_a is exceeded. The threshold force of these gap elements is related to the maximum force that the device is able to withstand. Furthermore, if the device is pushed beyond the point at which the axial force drops, the failure of bolts is expected. Once failure occurs, the system behaves as a bare frame. When the displacement of the system (friction-damped diagonal-bracing) at a time t_i is larger than a threshold value, u_a , the *MinMax* material defined in OpenSees is able to control the "switching off" phase of the device from the time t_i until the end of the analysis. This switching condition is simulated in the model by setting up the *MinMax* material to fail when the strain of the *ElasticPPGap* material exceeds the predefined bounds either in tension or compression, as shown in Fig. 2.5b. In this model, the *Steel02* material was assigned to the truss element and was employed to simulate the brace behavior in tension and compression. A kind of similar modelling technique was employed by Tong et al. (2011) to simulate the behavior of self-centering steel beam-column connections with bottom flange friction devices in OpenSees framework.

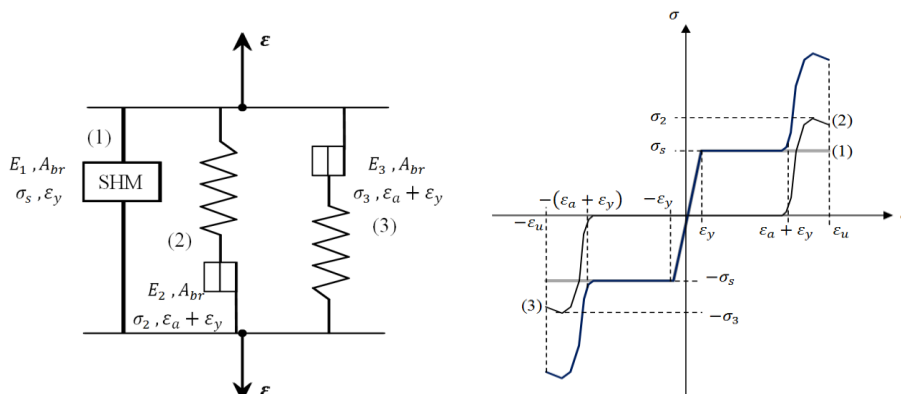


Figure 2.5. Equivalent material and the stress-strain curve used to define the friction damper installed in series with the diagonal-brace: (1) BoucWen material; (2), (3) ElasticPPGap combined with MinMax material

The proposed OpenSees model is used to simulate the behavior of a FDDB system shown in Fig. 2.6a. The brace element is loaded at joint j along the degree of freedom (DOF), u , by means of a quasi-static displacement, where the amplitudes of the loading protocol are given in terms of the available slip

distance, u_a , such as: 0.5, 0.75, 1, 1.5 and $2u_a$. The brace cross section corresponds to HSS 203x203x9.5 ($F_y = 350\text{MPa}$ and $E=200000\text{MPa}$). The slip force, P_s was chosen to preserve the elastic behavior of the brace in tension and compression ($P_s < 130\%C_r$), where C_r is the buckling strength of the truss member. In this example, $P_s = 600\text{ kN}$, the axial stiffness of the brace computed as $k_{br} = A_{br}E/L$ is equal to 144.2 kN/mm and the parameter used to set the BW model is $n = 10$ (computation is conducted in kN and mm). By using Eqn. 2.4, it conducts to $u_y = P_s/k_0$ and by equating the stiffness of damper to the stiffness of brace $k_o = k_{br}$ it leads to $u_y = 4.2\text{ mm}$. On the other hand, for the slip-lock model, the maximum expected force to be developed at bearing, f_{max} was set to be $f_{max} = 150\text{ kN}$. Based on setting verification: $f_{max} + P_s = 750\text{ kN} < C_r = 833\text{ kN}$, the elastic brace response is preserved. The input data for the slip-lock system was assumed to be: $u_a = 24\text{ mm}$, $u_b = 31\text{ mm}$, $u_c = 36\text{ mm}$, $f_b = 100\text{ kN}$, $f_c = 130\text{ kN}$ and $f_d = 150\text{ kN}$. From Fig. 2.6b is shown that the proposed FDB model is able to exhibit a smooth transition from the elastic to slipping stage, as well as a gradual transition at the neighboring of the slip limit ($u_a = 24\text{ mm}$) when the demand exceeds the slip distance.

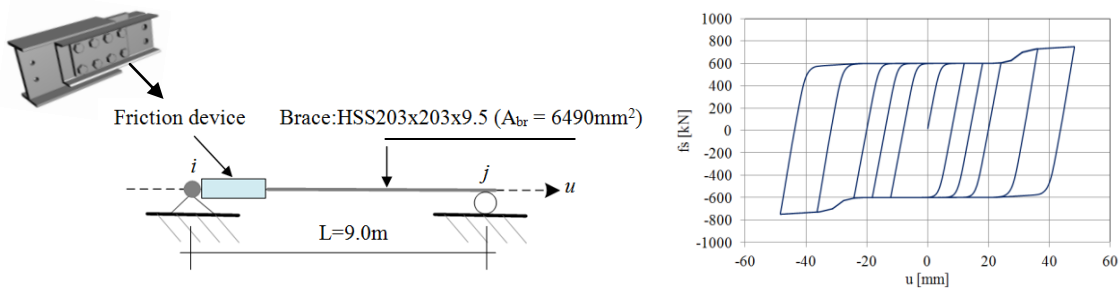


Figure 2.6. Hysteresis response of a friction-damped diagonal-bracing system using OpenSees

3. NUMERICAL SIMULATION OF 8-STOUREY MRF BUILDING EQUIPPED WITH FDBB

3.1 Building description

The selected 8-storey MRF office building is located on a firm soil in Montreal. The typical plan view and the OpenSees model are shown in Fig. 3.1. As illustrated, the seismic force resisting system in the E-W direction is composed of two moderately ductile moment resisting frames, MD-MRFs with three equal bays located along the external axes 1 and 6 and two similar MD-MRFs located in the N-S direction, along the gridlines B and E. The specified dead load at the roof and typical floor level is 3 kPa and 4.7 kPa respectively, while the snow load is 2.48 kPa. The specified live load is 2.4 kPa and for cladding 1.0 kPa is considered. The bare MD-MRF showed in Fig. 3.1 was designed with a ductility-related force modification factor, $R_d = 3.5$ and the overstrength factor $R_o = 1.5$. The rationale of employing a MD-MRF system is to emphasize the benefit of incorporating FDBB devices in moment frame building structures. These devices are able to preserve the structure in elastic range.

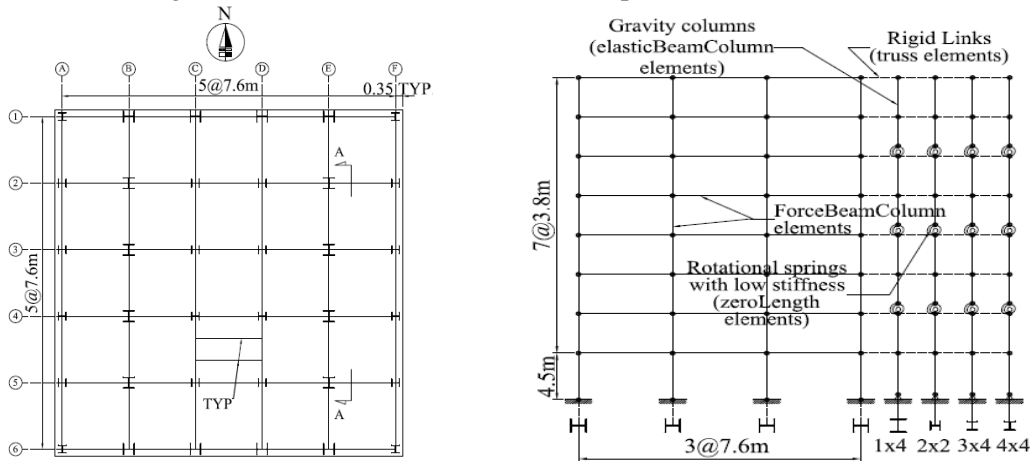


Figure 3.1. Typical plan view and the OpenSees model

The design of the MD-MRF system was conducted in accordance with the CSA/S16-2009 and NBCC 2010 provisions and the dynamic characteristics of the building structure are shown in Table 3.1.

Table 3.1. Fundamental period and seismic weight, W , of the 8-storey building

Building	h_n [m]	W [kN]	$T_a = 0.085(h_n)^{3/4}$ [s]	$T = 1.5T_a$ [s]
8-story	31.10	60855	1.12	1.68

The force-base nonlinear beam-column element object, *beamWithHinges*, with two-point Gauss-Radau integration scheme (Scott 2011) is used to model the beams and columns of MRFs. Members cross sections within the plastic hinge regions were discretized into fibers to account for the interaction between axial forces and bending moments. The web of W-shape cross section is divided in 32 fibers (16 along the web's depth) and each flange was divided in 64 fibers with 4 fibers along the flange thickness. The *Steel02* material with strain hardening following the Giuffre-Menegotto-Pinto model was assigned to the fibers of cross-sections and a 2% Rayleigh damping, was considered in the first and third vibration mode of the structure. In this analysis, the Newton algorithm was selected and the time step used for integration is 0.002, which is less or equal than the accelerogram time step. The computed fundamental period of this OpenSees model is $T_1 = 2.81$ s. To investigate the response of the 8-storey building equipped with FDDB devices, the OpenSees model was subjected to a set of 15 simulated records (Atkinson 2009) in the range of magnitude M6-M7 and different epicentral distances varying in the interval 11 km to 99 km. All selected ground motions (Morales Ramirez 2011) were scaled based on a procedure developed by Reyes and Kalkan (2011) to match the uniform hazard spectrum (UHS) for Montreal (2% in 50 years) within the interval $0.2T_1 - 1.5T_1$. The scaled acceleration spectra within the period of interest, the mean of the scaled ground motions and the UHS are shown in Fig. 3.2.

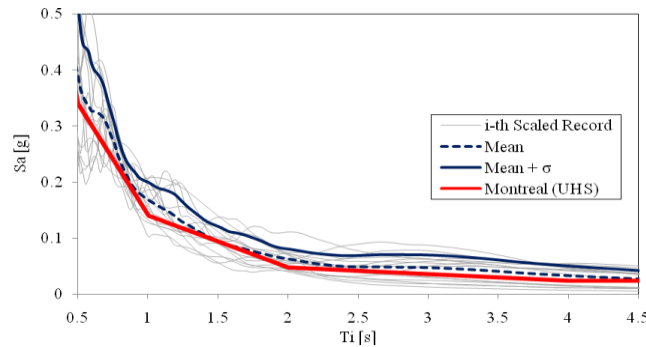


Figure 3.2. Scaled acceleration response spectra within the period of interest $0.2T_1 - 1.5T_1$

3.2 Seismic response of MD-MRF building structure equipped with FDDB

The need of adding damping to a MD-MRF structure is required either to preserve the MRF members in elastic range under seismic excitations or to prevent the failure of non-structural components (brick facades and others). The design methodology of MRF structures with FDDB devices consists of setting the number of FDDB devices per floor, the value of slip load and the selection of their location (Tirca et al. 2010). Essentially, this design process follows two steps: i) compute the optimum load activation of friction dampers per each floor and ii) select the optimum location of dampers in order to minimize the torsion effect. The slip load of each damper is computed by minimising the difference between the seismic input energy, E_I and the energy dissipated by dampers, E_h . This parameter depends mainly on the structure properties and the seismic demand. Herein, all MRF's members are protected from seismic damage, while dampers are designed to slip when the defined shear deflection is reached. As shown in Fig. 3.3, two different configurations of dampers locations are considered: scenario A (4 devices are installed at each floor) and scenario B (4 devices are installed at each alternative floor). The fundamental period corresponding to scenarios A and B is 1.33 s and 1.97 s, respectively. Regarding scenario A, the slip force computed at the ground floor level is 480 kN and it decreases until the 7th floor as follow: 420, 380, 350, 330 and 300 kN. The slip force at the upper two

floors is 300 kN. The mean and the 84 percentile (P84) of interstorey drift computed for the bare MD-MRF frame and the frame with devices under the 15 ground motions is shown in Fig. 3.3c.

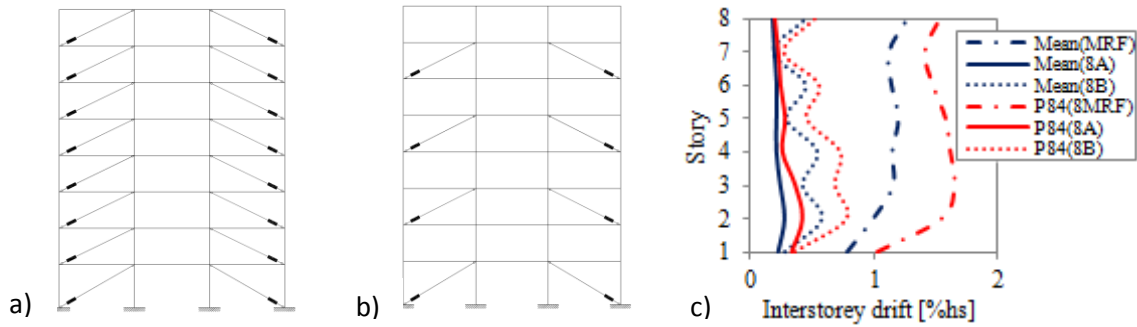


Figure 3.3. MD-MRF with different configurations of FDDB devices: a) case A; b) case B; c) interstorey drift

The roof time history displacement under record #10 is shown in Fig. 3.4 for the bare frame and for the frame equipped with FDDB devices. As illustrated, in both scenarios the last activation was recorded before $t = 14.0$ s while the total ground motion duration is 20 s. The hysteresis loop of the FDDB located at ground floor level is shown in Figure 3.4c for scenarios A and B. By considering the model of FDDB device without restraints, the maximum slip distance of 30 mm was recorded under ground motion #11 (Fig. 3.5). From numerical results, it is concluded that the demanded slip distance is an important parameter that controls the slip-lock phase. By providing larger slotted hole, the positive aspect of frame recentering is diminished. As illustrated in Fig. 3.5, in the case of scenario B, the mean of the demanded slip distance is 18 mm and the 130% of the mean slip distance is 24 mm which is in agreement with FEMA 356 requirements. When a slip distance defined as $u_{slip} = 2x(1.3u_a)$ is considered, bearing stage is experienced by FDDB device under records #8 and #11. It is assumed that braces remain elastic and failure of FDDBs occurred when the bearing force reaches the limit.

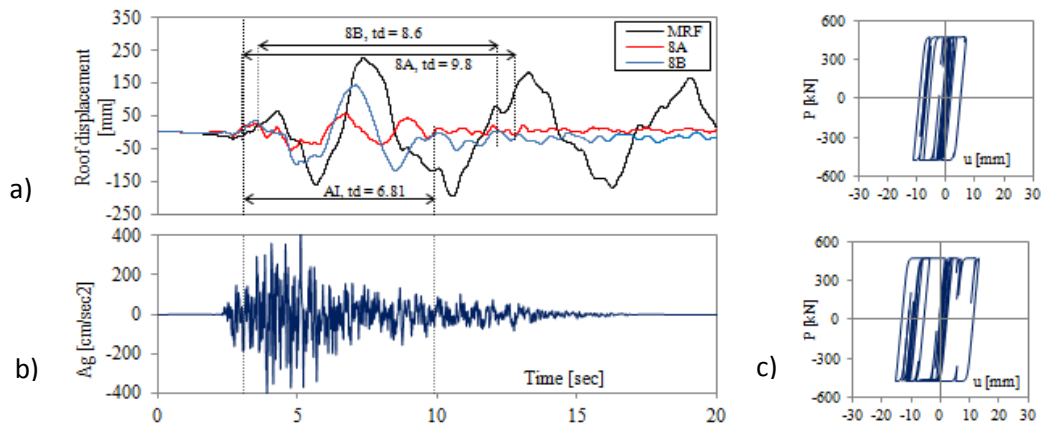


Figure 3.4. Roof displacement history of MD-MRF vs MD-MFR with FDDB devices: a) roof displacement histories b) accelerogram #10; c) hysteresis loop of devices located at GF level (scenario A and B)

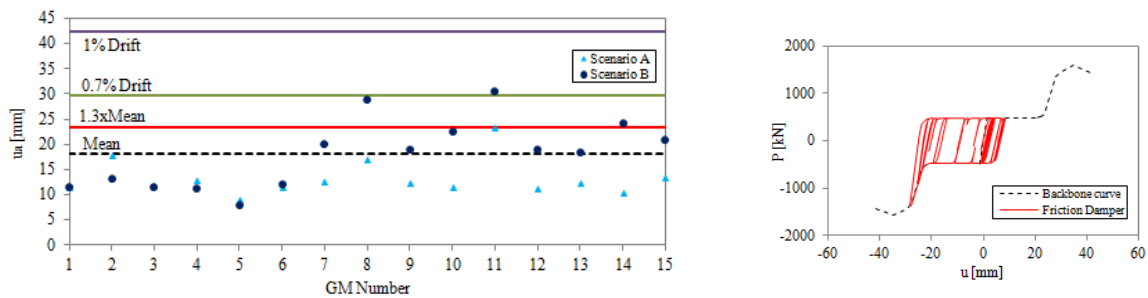


Figure 3.5. The computed slip distance u_a , (scenarios A and B) and the response of FDDB under GM #11.

4. CONCLUSIONS

An OpenSees model of Fddb device was developed. The uniaxial *BoucWen* material was selected to replicate the smooth hysteresis behavior of friction damper during the slipping stage. In addition, two sets of 3 bilinear gap springs arranged in parallel and characterized by the Elastic-Perfectly Plastic Gap material were added to simulate the slip-lock stage. Each set of *ElasticPPGap* material has a defined stress-strain or force-deformation relationship either in tension or in compression. The failure of device (decoupling) is simulated by setting up the *MinMax* material to fail when the strain of the *ElasticPPGap* material exceeds the predefined bounds either in tension or compression. In this model, *Steel02* material is assigned to brace member and force-base nonlinear beam-column element with concentrated plasticity were used to simulate the behavior of MRF's members.

From numerical analysis, it was found that the seismic response is influenced by: the number of devices per floor; the slip load; the length of slotted hole and the frequency content of ground motions. In this study, two Fddb models with and without restraints (*MinMax* material) were proposed. Herein, the demanded slip distance is computed from nonlinear time-history analysis by using 15 ground motions. Then, a slip distance equal to 130% of the mean calculated displacement in the device is assigned. It was observed that friction devices were activated at different time steps during the ground motion excitation. When the model with restraints is employed and the slip-lock phase occurs, the amount of damping and the fundamental period decrease, while the base shear increases.

REFERENCES

- Aiken, I.D., Nims, D., Whittaker, A. And Kelly, J.M. (1993). Testing of passive energy dissipation systems. *Earthquake Spectra, Earthquake Engineering Research Center*. University of California, Berkeley, Ca.
- Atkinson, G. (2009). Earthquake time histories compatible with the 2005 National building code of Canada uniform hazard spectrum. *Canadian Journal of Civil Engineering*. **Vol. 36: 6**, 991-1000.
- Bouc, R. (1967). Forced vibration of mechanical systems with hysteresis. *Fourth Conference on Nonlinear Oscillation, Prague, Czechoslovakia*.
- Canadian Standard Association. (2009). CAN/CSA-S16-09 Limit states design of steel structures. Canadian Standard Association, Toronto, ON.
- Federal Emergency Management Agency (FEMA). (2000). Prestandard and commentary for the seismic rehabilitation of buildings. FEMA-356, Washington, D.C.
- Foliente, G. (1993). Stochastic dynamic response of wood structural systems. PhD Thesis, Virginia Polytechnic Institute, Blacksburg, Virginia.
- Lukkunaprasit, P., Wanitkorkul, A. And Filiatrault, A. (2004). Performance deterioration of slotted-bolted connection due to bolt impact and remedy by restrainers. *Thirteen World Conference on Earthquake Engineering, Vancouver, B.C.* No. 1986.
- McKenna, F. and Fenves, G.L. (2004). Open System for Earthquake Engineering Simulation (OpenSees), PEER, University of California, Berkeley, CA.
- Morales Ramirez, J.D. (2011). Numerical simulations of steel frames equipped with friction-damped diagonal-bracing devices. MAsc Thesis, Building, Civil and Env. Eng., Concordia University, Montreal, QC.
- Reyes, J.C. and Kalkan E. (2011). Required number of records for ASCE/SEI 7 ground motion scaling procedure. U.S. Geological Survey Open-File Report 2011-1083.
- Pall, A. (1979). Limited slip bolted joints, a device to control the seismic response of large panel structures. PhD Thesis, Building, Civil and Environmental Engineering, Concordia University, Montreal, QC.
- Pall, A. and Marsh, C. (1981). Response of friction damped braced frames. *Journal of Structures Division, ASCE*. **Vol. 108: ST6**, 1313-1323.
- Roberts, J. and Spanos, P. (1990). Random vibration and statistical linearization. Jhon Wiley & Sons Ltd.
- Roik, K., Dorka, U. And Dechent, P. (1988). Vibration control of structures under earthquake loading by three-stage friction-grip elements. *Earthquake Eng. and Struct. Dynamics, J. Wiley & Sons Ltd*. **Vol 16**, 501-521.
- Tirca, L, Morales Ramirez, J.D., Guo, G.L. and Chen, L. (2010). Optimal design of friction dampers for multi-storey buildings. *9th US national and 10th Canadian Conf. in Earthquake Engineering*, Toronto, On.
- Tong, G., Lianglong, S. and Guodong, Z. (2011). Numerical simulation of the seismic behavior of self-centering steel beam-column connections with bottom flange friction devices. *Earthquake Engineering and Eng. Vibration* **10:2**, 229:238.
- Wen, Y-K. (1980). Equivalent linearization for hysteretic systems under random excitation. *Journal of Applied Mathematics, ASME* **47**, 150-154.